Research Square

Preprints are preliminary reports that have not undergone peer review.
They should not be considered conclusive, used to inform clinical practice,
or referenced by the media as validated information.

Plasmalogen deficiency and purinergic stress define three metabolic axes in schizophrenia

Nikita Basov
nikita.v.basov@gmail.com
Westlake University https://orcid.org/0000-0001-6390-5796
Polina Brit
Maria Lysenko
Maria Sotnikova
Disa Tekueva
Zaira Kharaeva
Artem Rogachev
Novosibirsk State University, N. N. Vorozhtsov Institute of Organic Chemistry, Novosibirsk, Russia https://orcid.org/0000-0002-3338-8529
Svetlana Morozkina
Diana Shorova
Westlake University
Jiaxiang Ding
Valentina Buneva
Evgeny Ermakov
Institute of Chemical Biology and Fundamental Medicine https://orcid.org/0000-0002-1084-6419
Huan Zhou
Dmitry Shcherbakov

Article

Keywords:

Posted Date: July 21st, 2026

DOI: https://doi.org/10.21203/rs.3.rs-10343202/v1

License: This work is licensed under a Creative Commons Attribution 4.0 International License. Read Full License

Additional Declarations: The authors have declared there is **NO** conflict of interest to disclose

Abstract

Plasma metabolomics has identified candidate biomarkers of schizophrenia, but most studies report group differences without separating disease-associated signals from antipsychotic exposure and symptom severity. We aimed to test whether targeted plasma metabolomics combined with pathway and gene-network annotation could partition metabolomic variation in schizophrenia into biologically interpretable components. Plasma from 41 inpatients with paranoid schizophrenia in acute exacerbation and 40 community controls was profiled using targeted liquid chromatography–tandem mass spectrometry covering 171 metabolites. Group differences were assessed with false discovery rate control and adjustment for age, sex and smoking, followed by exploratory classification, correlation-network, clinical-scale and subgroup analyses. Plasmalogen p16:0/20:4 was the only metabolite that survived covariate-adjusted false discovery rate correction. Its single-metabolite classification performance was close to that of multivariate models, with an area under the receiver operating characteristic curve of 0.838. Pathway enrichment and metabolite-to-enzyme-to-gene mapping converged on glycerophospholipid metabolism and Lands-cycle enzymes, with LPCAT4, PLA2G4A and LPCAT1 showing the highest schizophrenia association scores among mapped phospholipid-remodelling genes. Subgroup and clinical-scale analyses suggested xanthine as a candidate severity-associated purinergic marker, whereas pyruvate, mevalonate and dimethyl-L-arginine were more consistent with antipsychotic-exposure-associated metabolic variation. These findings support a working model in which plasma metabolomic variation in schizophrenia can be partially partitioned into phospholipid-remodelling, antipsychotic-exposure-associated and purinergic-stress-related components. This model warrants replication in larger, longitudinal and drug-naive cohorts.

1. Introduction

Schizophrenia (SCZ) is a heterogeneous polygenic disorder in which positive, negative, and cognitive symptom domains do not map cleanly onto distinct biological signatures, and in which clinical response, side-effect burden and cognitive trajectory remain difficult to predict at the individual patient level (1–4). Plasma metabolomics offers a tractable readout of this heterogeneity because the small-molecule pool integrates peripheral metabolism, gut microbiota, antipsychotic exposure and central nervous-system neuroactive substrates without requiring invasive sampling (3–6).

Over the past three years, three convergent lines of evidence for metabolomic alterations in SCZ have emerged. First, glycerophospholipid and plasmalogen lowering has been reported in medication-naïve(1, 7, 8) chronic and treated SCZ(9, 10) early-onset disease(11) and psychiatric comparator cohorts (1, 10, 12); the Tkachev et al. multicenter study identified 77 reproducible lipids with cross-cohort classification AUC of 0.86–0.95(9). Second, kynurenine-pathway shifts, including altered quinolinic acid, kynurenic acid, free tryptophan and QUIN/KYNA ratio, have been replicated in first-episode plasma (13), long-term-treated patients (14, 15), postmortem dorsolateral prefrontal cortex(16) and cerebrospinal-fluid meta-analyses(17), with high baseline KYNA linked to antipsychotic non-response in one study (18). Third, purinergic and oxidative-stress markers, particularly xanthine, hypoxanthine and uric acid, are repeatedly altered in SCZ blood and have been linked to xanthine-oxidase activity, glutathione depletion and potential XO inhibitor adjunctive strategies (19–22).

These findings remain insufficient for clinical translation because three methodological gaps persist. First, disease-related signals are entangled with antipsychotic exposure: inpatient SCZ cohorts in exacerbation are usually medicated, and antipsychotics reshape mitochondrial respiration, electron transport chain (ETC) activity, including complex I activity, lipid biosynthesis, autophagy and the tryptophan–kynurenine axis (23–30). Specific examples include complex-I inhibition by aripiprazole, brexpiprazole and cariprazine(26), olanzapine-related lysosomal/autophagy stress (29), clozapine-associated AhR–tryptophan–kynurenine metabolic effects (31) and second-generation antipsychotics have been implicated in disruption of oxidative phosphorylation, tricarboxylic acid (TCA) and glycolytic programmes (24). Second, smoking confounds the lipid signal: it is more prevalent in SCZ and can lower phosphatidylcholine and plasmalogen levels independently of psychiatric disease. Third, metabolomic reports rarely link altered metabolites to catalysing enzymes, gene symbols and interaction partners, although such mapping can connect metabolic findings to schizophrenia-associated loci (32–34). This is particularly relevant for PLA2G4A, implicated by CNV data in SCZ symptom dimensions(35) and for LPCAT enzymes involved in Lands-cycle glycerophospholipid re-acylation and ferroptosis-relevant lipid remodelling (36–40).

We address these gaps in a discovery cohort of 41 paranoid SCZ inpatients in acute exacerbation and 40 community controls profiled by hydrophilic interaction liquid chromatography–tandem mass spectrometry with multiple reaction monitoring (HILIC LC–MS/MS MRM) using a panel of 171 unique metabolites after quality control (QC) filtering. Rather than pre-selecting a shortlist, we combine FDR-controlled univariate testing with covariate adjustment, regularised multivariate classification, within-group correlation networks, KEGG/SMPDB enrichment against the panel-detectable background, metabolite → enzyme → gene STRING mapping with Open Targets SCZ annotation(33), partial correlations with clinical scales and chlorpromazine-equivalent dose (CPZeq), and explicit case-vs-case deconfounding contrasts. The aim is not to propose a deployable diagnostic biomarker panel, but to test whether plasma metabolomics can separate disease-related, antipsychotic-related and severity-related signals and map them onto plausible biochemical mechanisms.

2. Materials and methods

2.1 Participants and clinical characterization

Forty-one inpatients with schizophrenia (ICD-10 F20.0) in acute exacerbation were recruited at the Republican Clinical Centre of Psychiatry and Narcology, Ministry of Health of the Kabardino-Balkarian Republic, Nalchik, Russian Federation. Forty community controls were recruited from the

same region. At the time of sampling, all patients with schizophrenia were receiving stable antipsychotic therapy. The study protocol was approved by the Local Ethics Committee of the Medical Academy of Kabardino-Balkarian State University named after H.M. Berbekov (expert conclusion No. 02.012, February 2, 2026). The study was conducted in accordance with the Declaration of Helsinki. Written informed consent was obtained from all participants and/or their legal representatives before enrolment.

Eighteen of 41 patients were female (44%); 30 of 40 controls were female (75%; Fisher's exact p = 0.0065). Mean age was 45.3 ± 11.4 years in SCZ and 39.3 ± 13.1 in controls (Welch's t = 2.20, p = 0.031). Both imbalances are imperfectly matched by design and are explicitly modelled as covariates in all confirmatory analyses (Section 2.5). For SCZ patients we recorded the Positive and Negative Syndrome Scale (PANSS)(41); the Brief Psychiatric Rating Scale (BPRS) (42); the Montreal Cognitive Assessment (MoCA) (43); the Montgomery–Åsberg Depression Rating Scale (MADRS) (44); the Snaith–Hamilton Pleasure Scale (SHAPS) (45); chlorpromazine-equivalent daily dose (CPZeq); antipsychotic class (typical vs. atypical); clozapine status (yes/no); polytherapy (yes/no); age of onset; illness duration; therapy duration and treatment response, assessed by the treating psychiatrists based on clinical judgement and documented improvement during inpatient treatment. The full clinical summary is presented in Table S1.

2.2 Sample preparation and LC–MS/MS analysis

Plasma sample preparation was carried out according to Li et al. (46). Briefly, 400 µL of a chilled MeOH–ACN mixture (1:1, v/v) was added to 100 µL of blood plasma, vortexed, shaken for 15 min, and centrifuged at + 4°C and 16,000 rpm for 15 min. The supernatants were transferred to plastic vial inserts and analysed by targeted LC–MS/MS; each sample was injected twice. Chromatographic separation was performed on a perfectSil 100 NH2 column (250 × 4.6 mm, 5 µm) under HILIC conditions using an LC-20AD Prominence system (Shimadzu, Kyoto, Japan) with a SIL-20AC autosampler thermostated at 10°C. Mass spectrometric detection was performed in MRM mode with positive/negative ion polarity switching on an API 6500 QTRAP (AB SCIEX, Framingham, MA, USA) equipped with an ESI source. The precursor and fragment ion transitions were partially adapted from Li et. al (46) and partially established in-house by direct infusion of pure reference standards. Full sample preparation details, LC–MS/MS parameters and MRM transition tables are provided in Supplementary methods S1–S2; sample identifier reconciliation is described in S3.

2.3 Pre-processing and QC

Raw transitions were filtered as follows: (1) median QC relative standard deviation (RSD) < 30%; (2) per-feature missingness < 20% across samples; (3) merging of MRM transitions to the same compound; (4) k-nearest-neighbour (k = 3) imputation of remaining missing values within group. After preprocessing, the dataset comprised 171 unique metabolites across 81 plasma samples. Two parallel scaled tables are retained: a QC-normalised table (per-feature mean = 1, used to report effect sizes on the natural scale) presented in Table S2 and a Pareto-scaled table (mean-centred, divided by √SD, used for all multivariate and network analyses) presented in Table S3.

2.4 Univariate testing

For each of the 171 metabolites we computed: (1) Welch's t-test, (2) Mann–Whitney U as a non-parametric robustness check, (3) Bayes factor BF_{10} (Rouder's default Cauchy prior on standardised effect, zero-centred Cauchy distribution with a scaling parameter of √2/2), (4) Cohen's d with bootstrap (5,000 iterations) 95% confidence interval, (5) Benjamini–Hochberg (BH) FDR over all 171 tests separately for the Welch and the Mann–Whitney statistics. To control for the sex–age–smoking imbalance between groups, every metabolite was additionally entered into a linear model [metabolite ~ group + age + sex + smoking] and the adjusted group coefficient β plus a BH-corrected adjusted FDR was retained.

2.5 Multivariate analysis and classification

Principal component analysis was performed on the Pareto-scaled matrix; score and loading plots were generated for the PC 1 – PC 4 components. PLS-DA and classifiers were trained on the 153-metabolite classification panel after dropping features with ≥ 20% missingness and within-group KNN imputation (k = 3); R^2Y and a 5-fold cross-validated Q^2Y were evaluated against a 1,000-permutation null distribution of the group label. For classification, we trained (1) a LASSO logistic regression with two regularisation regimes – default (λ chosen by the 1-SE rule; ~65 features retained on median) and sparse (λ pushed down to retain ~ 32 features), (2) a Random-Forest classifier with 500 trees, both under stratified 5-fold cross-validation. AUCs are reported as mean ± SD across folds. Observed AUCs were compared with a 1,000-permutation null distribution of group labels.

2.6 Correlation network and differential correlation

Within-group Spearman correlation matrices were computed separately for the SCZ and control groups. Edge significance was assessed by BH FDR over all pairs. We retained edges with within-group $|\rho| \geq 0.5$ and FDR < 0.05. Differential-correlation analysis compared the Fisher z-transformed correlations between groups, and edges were classified as SCZ-only, control-only or shared according to which group(s) they were significant in. Louvain community detection was performed on the union network using v. 0.16 python-louvain library (modularity-maximising partition; seven communities retained).

2.7 KEGG/SMPDB enrichment

Each metabolite was mapped to KEGG compound IDs and HMDB IDs via automated parsing followed by manual curation of ambiguous lipid species (notably the phosphatidylcholine / phosphatidylinositol / plasmalogen species, for which we used the headgroup-level identifier when the precise sn-1/sn-2 mapping was ambiguous). Over-representation was tested by hypergeometric distribution against the panel-detectable background (n = 126

metabolites mapped to ≥ 1 KEGG pathway), not against the full human metabolome – a correction intended to avoid spurious pathway-enrichment hits that avoids spurious "all lipid pathways significant" hits. Permutation-based pathway enrichment (1,000 permutations of metabolite labels) provided an additional empirical FDR.

2.8 Metabolite, enzyme and gene STRING network

For each significantly altered metabolite (n = 17 across BF_AND_d, combined_any, and disease_only labels) we extracted the catalysing enzymes by EC number from KEGG REACTION and HMDB protein associations. The EC numbers were expanded to human gene symbols (HUGO) by KEGG hsa mappings, yielding 116 enzyme records collapsing to 99 unique HUGO gene symbols. Gene–gene interactions were queried in STRING v12 with a high-confidence threshold (score ≥ 0.7), yielding a 455-edge subnetwork clustered by Leiden modularity (ModularityVertexPartition, seed = 42). All genes were annotated with (a) the direction of change of the connected metabolite, (b) the Open Targets schizophrenia association score (if available), and (c) the Leiden module membership.

2.9 Continuous clinical-scale correlations

Within SCZ only, Spearman correlations were computed between each of the 171 metabolites and each of PANSS_total, PANSS_positive, PANSS_negative, PANSS_general, BPRS_total, MoCA_total, MADRS_total, SHAPS_total, CPZeq dose, age and illness_duration. BH FDR was applied per scale and an alternative global FDR was reported for transparency. Partial Spearman correlations with the same scales were then computed, adjusting for sex, age, smoking and (where appropriate) CPZeq dose, so that a finding labelled "PANSS-associated" survives controlling for drug dose.

2.10 Subgroup deconfounding

Twelve case-vs-case contrasts within the SCZ arm were run with FDR over the 171 metabolites and with covariate adjustment: smoking (Yes vs No), antipsychotic class class (Typical vs Atypical), clozapine (Yes vs No), polytherapy (Poly vs Mono), CPZeq dose (High vs Low tertile), response (Yes vs No), onset (Early vs Late), and four symptom-domain bins (PANSS-high vs PANSS-low, BPRS-high vs BPRS-low, MoCA-impaired vs normal, MADRS-severe vs mild) and a positive vs negative-symptom contrast. The metabolite × subgroup signed effect-size matrix (Fig. 3) was hierarchically clustered to expose which signals are shared across subgroups vs subgroup-specific.

2.11 Software and reproducibility

All analyses were performed in Python 3.11 (pandas 2.2, scikit-learn 1.5, scipy 1.13, statsmodels 0.14, networkx 3.3, matplotlib 3.9, seaborn 0.13). KEGG queries were performed against KEGG REST as of 2025-Q4. STRING (v12.5) was queried via the public REST API. OpenTargets was queried via the public GraphQL API with the schizophrenia MONDO ID = MONDO_0005090. A reproducibility note, full parameter values and software versions are deposited in the Supplementary methods.

3. Results

3.1 Cohort, panel and quality control

Forty-one patients with schizophrenia in acute exacerbation and 40 community controls passed sample QC and contributed to the analysis. Clinical characteristics are summarized in Table S1. The SCZ arm had a higher proportion of males than the control group (56% vs 25%; Fisher's exact p = 0.0065), and mean age differed by 6.0 years (45.3 ± 11.4 vs 39.3 ± 13.1 years; Welch's t = 2.20, p = 0.031). Smoking was more frequent in SCZ than in controls: 15/41 patients (37%) versus 6/40 controls (15%; Fisher's exact test, OR = 3.27, p = 0.0415). These variables were therefore included as covariates in adjusted models.

Of the 215 raw MRM transitions, all retained adequate QC across the 81 plasma samples. Merging of quantifier/qualifier transitions reduced the panel to 171 unique metabolites. Median per-feature missingness was below 5%; nine metabolites with 5–20% missingness were imputed by within-group KNN (k = 3). The cleaned 171-metabolite panel formed the analytic dataset for all subsequent analyses.

3.2 Univariate FDR-controlled differential metabolites

After BH correction over all 171 metabolites, five metabolites passed the BH-FDR < 0.05 threshold in unadjusted Welch testing (Table 1; Fig. 1a,b). These were dominated by glycerophospholipid-related and lipid-associated signals, with the strongest effect observed for plasmalogen (p16:0/20:4) (d = − 1.19, 95% CI − 1.66 to − 0.79, BF10 = 1.3 × 10^4), followed by phosphatidylcholine (16:0/18:2), phosphorylcholine, 2-octenoylcarnitine and cholesterol.

Table 1
Top 20 differential metabolites in SCZ compared with controls: raw Cohen's d, BF_{10}, BH-FDR over 171 metabolites, and age-, sex- and smoking-adjusted; adjusted β and FDR.

Metabolite	mean SCZ	mean Control	Cohen's d (95% CI)	BF_{10}	Welch p (uncorr.)	BH-FDR (univariate)	$B_{adj.}$	$p_{adj.}$	FDR_{adj}
Plasmalogen (p16:0/20:4)	-243.8	231.6	-1.19 (-1.66, -0.79)	$1.3\times10^{+4}$	1.4×10^{-6}	0.000	-376.62	1.8×10^{-4}	0.030
PC (16:0/18:2)	-604.8	619.9	-1.06 (-1.54, -0.65)	$1.8\times10^{+3}$	1.2×10^{-5}	0.001	-992.08	7.9×10^{-4}	0.067
Phosphorylcholine	-562.4	449.9	-0.91 (-1.42, -0.48)	$1.3\times10^{+2}$	1.8×10^{-4}	0.010	-753.89	6.7×10^{-3}	0.285
2-Octenoylcarnitine	-236.1	242.0	-0.75 (-1.24, -0.32)	25	1.3×10^{-3}	0.048	-413.59	1.0×10^{-2}	0.351
Cholesterol	-166.6	136.7	-0.78 (-1.32, -0.34)	23	1.4×10^{-3}	0.048	-246.84	1.7×10^{-2}	0.381
PI (38:4)	-232.1	232.1	-0.71 (-1.35, -0.24)	15	2.3×10^{-3}	0.064	-367.01	2.4×10^{-2}	0.381
Xanthine	108.5	-111.2	0.65 (0.31, 1.04)	8.7	4.8×10^{-3}	0.118	211.24	1.5×10^{-2}	0.381
Tryptophan	-285.0	292.1	-0.63 (-1.07, -0.20)	6.4	6.5×10^{-3}	0.140	-519.82	2.7×10^{-2}	0.381
PI (38:3)	-97.6	85.4	-0.60 (-1.19, -0.14)	4	1.2×10^{-2}	0.213	-133.07	8.9×10^{-2}	0.562
Asparagine	-351.9	360.7	-0.58 (-0.94, -0.20)	3.8	1.3×10^{-2}	0.213	-564.09	6.6×10^{-2}	0.562
Indole	-210.4	215.6	-0.56 (-1.03, -0.17)	3.5	1.4×10^{-2}	0.213	-366.21	5.5×10^{-2}	0.562
Nicotinic acid	-35.1	36.0	-0.54 (-0.92, -0.12)	2.8	1.9×10^{-2}	0.261	-75.79	2.5×10^{-2}	0.381
SAH	49.8	-53.7	0.52 (0.09, 1.00)	2.4	2.2×10^{-2}	0.261	56.55	2.4×10^{-1}	0.718
1-Methylnicotinamide	192.3	-197.1	0.52 (0.37, 1.11)	2.5	2.2×10^{-2}	0.261	424.32	2.3×10^{-2}	0.381
Hypoxanthine	208.1	-213.3	0.51 (0.30, 0.81)	2.4	2.4×10^{-2}	0.261	629.82	2.1×10^{-3}	0.119
Purine	-87.2	89.4	-0.50 (-0.93, -0.06)	2.1	2.7×10^{-2}	0.261	-159.18	7.3×10^{-2}	0.562
PI (36:2)	-57.9	40.1	-0.54 (-1.03, -0.07)	2.1	2.8×10^{-2}	0.261	-54.2	2.6×10^{-1}	0.718
L-Tryptophan	-1174.3	1203.7	-0.50 (-0.93, -0.09)	2	2.8×10^{-2}	0.261	-2021.19	9.2×10^{-2}	0.562
L-Threonine	-186.0	190.7	-0.49 (-0.92, -0.10)	1.9	3.0×10^{-2}	0.261	-264.5	1.6×10^{-1}	0.644

Abbreviations: BF10 – the Bayes factor, BH-FDR – the Benjamini-Hochberg False Discovery Rate correction, FDRadj – sex/age/smoking-adjusted False Discovery Rate corrected p-values, PC – phosphatidylcholine, PI – phosphatidylinositol, SAH – S-Adenosyl-L-homocysteine.

Metabolite	mean SCZ	mean Control	Cohen's d (95% CI)	BF_{10}	Welch p (uncorr.)	BH-FDR (univariate)	$B_{adj.}$	$p_{adj.}$	FDR_{adj}
Creatine	-1619.9	1660.4	-0.49 (-0.93, -0.09)	1.9	3.1×10^{-2}	0.261	-2169.94	1.8×10^{-1}	0.696

Abbreviations: BF10 – the Bayes factor, BH-FDR – the Benjamini-Hochberg False Discovery Rate correction, FDRadj – sex/age/smoking-adjusted False Discovery Rate corrected p-values, PC – phosphatidylcholine, PI – phosphatidylinositol, SAH – S-Adenosyl-L-homocysteine.

After adjustment for age, sex and smoking, only plasmalogen p16:0/20:4 survived panel-wide FDR correction (βadj. = −377, adjusted FDR = 0.030; Table 1; Fig. 1a,b). Hypoxanthine had an adjusted FDR < 0.15, whereas PC(16:0/18:2), phosphorylcholine, PI(38:4) and other lipid hits attenuated after covariate adjustment. Xanthine showed a positive disease effect at the uncorrected level (β = +211, p = 0.015) but did not survive panel-wide FDR (FDRadj. = 0.38).

3.3 PCA, PLS-DA and cross-validated classification

The first principal component of the Pareto-scaled matrix captured 39.8% of total variance and correlated strongly with the per-sample row sum (r = 0.96; Fig. 1c), consistent with a non-biological global-signal axis. Group separation was instead driven by PC4 (6.3% of variance; group r = − 0.40; Fig. 1d). Two-component PLS-DA on the 153-metabolite panel showed supervised group separation (R^2Y = 0.476, Q^2Y = 0.315; 1,000-permutation p < 0.001 for both metrics; Fig. 1e and Fig. 2b).

Classifier performance is summarized in Fig. 2a,c. Random Forest achieved the highest 5-fold cross-validated AUC (0.858), followed by PLS-DA (0.852), LASSO logistic regression and the single-metabolite plasmalogen p16:0/20:4 model (AUC = 0.838). Feature stability and Random-Forest rankings are provided in Table S4. Given the modest sample size, these models are reported as discovery-phase discrimination analyses rather than deployable diagnostic classifiers.

3.4 Correlation rewiring across metabolic axes and subgroup deconfounding

We next compared within-group Spearman correlation structures between schizophrenia and controls to test whether altered metabolites also showed disease-associated network rewiring (Fig. 3a–f). Within the disease-associated phospholipid axis, 8 of 66 pairwise correlations were stronger in schizophrenia than in controls at uncorrected p < 0.05, and all eight showed positive Δρ. No pair survived FDR correction across the 66 tests, but the concordant direction of effects supported tighter phospholipid co-regulation in schizophrenia (binomial p = 0.004). The strongest examples included PC(16:0/18:2)–PI (36:2) (ρSCZ = + 0.95, ρCtrl = + 0.82, Δρ = +0.12, p = 0.013) and PI (38:3)–PI (36:1) (Δρ = +0.28, p = 0.015; Fig. 3e,f).

Cross-axis correlations pointed to coupling between phospholipid and mitochondrial-fuel signals. PI(38:5) gained a positive correlation with pyruvic acid in schizophrenia (ρSCZ = + 0.47, ρCtrl = − 0.32, Δρ = +0.79, p = 0.002; Fig. 3a), while mevalonic acid and L-acetylcarnitine became more strongly coupled in schizophrenia than in controls (ρSCZ = + 0.55, ρCtrl = + 0.03, Δρ = +0.52, p = 0.036; Fig. 3c). Conversely, xanthine and pyruvic acid showed weaker coupling in schizophrenia than in controls (ρSCZ = + 0.21, ρCtrl = + 0.68, Δρ = −0.48, p = 0.007; Fig. 3b), and the 1-methylnicotinamide–allantoin association was also reduced (ρSCZ = + 0.09, ρCtrl = + 0.68, Δρ = −0.59, p = 0.043; Fig. 3d).

Subgroup deconfounding within the schizophrenia arm further supported separation of disease-associated, antipsychotic-exposure-associated and severity-associated signals (Fig. 3h). Across the 5,779 edges in the union network, panel-wide differential-correlation analysis yielded five edges at differential-correlation FDR < 0.05. The strongest was a gain-of-edge allantoin–PI(38:5) correlation in schizophrenia (ρSCZ = + 0.79, ρCtrl = − 0.36, diff-FDR = 4 × 10 − 6), linking oxidative-damage and phospholipid- remodelling signals. Full edge-level results, subgroup contrasts and hub-metabolite statistics are provided in Table S3.

3.5 Metabolite → enzyme → gene network with OpenTargets schizophrenia overlay

Pathway over-representation was tested against the panel-detectable KEGG background (n = 126 mapped metabolites). The leading signal was glycerophospholipid metabolism (KEGG map00564), with 5 of 13 panel-detectable members represented among the altered metabolites: PC(16:0/18:2), PI(38:3), PI(38:4), PI(36:2) and phosphorylcholine (fold enrichment = 4.85, hypergeometric p = 0.0010, hypergeometric FDR = 0.012; Table 2; Fig. 4a). Choline metabolism in cancer (map05231) was the second strongest pathway-level signal, driven by PC(16:0/18:2) and phosphorylcholine (2/3 members, fold enrichment = 8.4, hypergeometric p = 0.016; Table 2; Fig. 4a). Lower-ranked but biologically coherent hits included tryptophan-related pathways, arachidonic-acid metabolism and caffeine metabolism, the latter driven by xanthine.

Table 2
Pathway enrichment analysis (KEGG, panel-detectable background, n = 126): hypergeometric p, hypergeometric FDR, 1,000-permutation p and FDR. Full information provided in Table S3, «Pathway Enrichment» sheet.

KEGG ID	Pathway	Metabolites in pathway	Hits / expected	Fold enrich.	Hypergeom. p	Hypergeom. FDR	Perm p	Perm FDR	Presented metabolites
map00564	Glycerophospholipid metabolism	13	5 / 1.03	4.85	0.001	0.012	0.002	0.110	PC (16:0/18:2); PI (38:3); PI (38:4); PI (36:2); Phosphorylcholine
map05231	Choline metabolism in cancer	3	2 / 0.24	8.4	0.016	0.304	0.000	0.000	PC (16:0/18:2); Phosphorylcholine
map00996	Biosynthesis of various alkaloids	4	2 / 0.32	6.3	0.031	0.387	0.006	0.220	Cholesterol; Tryptophan
map00400	Phenylalanine, tyrosine and tryptophan biosynthesis	7	2 / 0.56	3.6	0.096	0.605	0.031	0.682	Indole; Tryptophan
map00380	Tryptophan metabolism	9	2 / 0.71	2.8	0.151	0.605	0.076	0.782	Indole; Tryptophan
map00901	Indole alkaloid biosynthesis	2	1 / 0.16	6.3	0.153	0.605	–	–	Tryptophan
map00590	Arachidonic acid metabolism	2	1 / 0.16	6.3	0.153	0.605	–	–	PC (16:0/18:2)
map00984	Steroid degradation	2	1 / 0.16	6.3	0.153	0.605	–	–	Cholesterol
map00232	Caffeine metabolism	2	1 / 0.16	6.3	0.153	0.605	–	–	Xanthine
map00999	Biosynthesis of various plant secondary metabolites	11	2 / 0.87	2.29	0.212	0.605	0.114	0.782	Indole; Tryptophan
map05143	African trypanosomiasis	3	1 / 0.24	4.2	0.221	0.605	0.025	0.682	Tryptophan
map00120	Primary bile acid biosynthesis	3	1 / 0.24	4.2	0.221	0.605	0.079	0.782	Cholesterol

Note: Hypergeometric p, hypergeometric FDR, 1,000-permutation p, and 1,000-permutation FDR are presented. Full information provided in Table S3, «Pathway Enrichment» sheet. Abbreviations: KEGG ID – the Kyoto Encyclopedia of Genes and Genomes (KEGG) identifier, FDR – False Discovery Rate correction, PC – phosphatidylcholine, PI – phosphatidylinositol.

The altered metabolites were then mapped to catalysing enzymes and human genes using KEGG and HMDB annotations. This yielded 116 enzyme records collapsing to 99 unique HUGO gene symbols. STRING analysis at a high-confidence threshold (score ≥ 0.7) generated a 455-edge interaction subnetwork (Fig. 4b). When annotated with Open Targets schizophrenia association scores, the highest-ranking glycerophospholipid-pathway genes were LPCAT4, PLA2G4A and LPCAT1, all linked to phosphatidylcholine remodelling. This convergence is consistent with independent CNV evidence for PLA2G4A involvement in schizophrenia symptom dimensions(35) and with recent literature on Lands-cycle re-acylation (36–40). Full pathway-enrichment and gene-network results are provided in Table S3.

3.6 Continuous clinical-scale correlations

Within the schizophrenia group, partial Spearman correlations were computed between each of the 171 metabolites and clinical variables, adjusting for sex, age, smoking and, where appropriate, CPZeq dose (Fig. 3g). Across 2,052 metabolite–scale tests, no association survived global FDR correction. At the exploratory level, 143 associations had uncorrected $p < 0.05$, and three associations reached FDR < 0.10 within individual scales: glutamic acid with therapy duration ($\rho = -0.52$, FDR = 0.085), pyruvic acid with age ($\rho = -0.52$, FDR = 0.073) and cytidine monophosphate with age ($\rho = +0.53$, FDR = 0.073).

Among PANSS-positive correlations, the strongest exploratory signals were positive associations with acylcarnitines, including 2-octenoylcarnitine ($\rho = +0.47$), pimelylcarnitine ($\rho = +0.44$), L-acetylcarnitine ($\rho = +0.42$) and octanoylcarnitine ($\rho = +0.42$). This pattern is consistent with reported antipsychotic-related shifts in fatty-acid β-oxidation [10, 46]. Across the SHAPS anhedonia scale, the dominant exploratory negative correlations

involved phospholipid-related species, including PI(36:4), PI(38:4), PC(16:0/18:2), nicotinamide riboside and myristoylcarnitine. These exploratory patterns are shown in Fig. 3g and detailed in Table S3.

4. Discussion

In this discovery cohort of 41 schizophrenia inpatients in acute exacerbation and 40 community controls, FDR-controlled and covariate-adjusted analysis of 171 plasma metabolites identified a concise and biologically interpretable metabolomic pattern. Plasmalogen (p16:0/20:4) was the only metabolite that survived panel-wide FDR correction after adjustment for sex, age and smoking, and its single-metabolite AUC approached that of multivariate classifiers. Metabolite-to-gene network analysis converged on glycerophospholipid-cycle enzymes, particularly LPCAT4, PLA2G4A and LPCAT1. Subgroup deconfounding further suggested that the broader metabolomic signal could be partially partitioned into putative disease-related, antipsychotic-exposure-related and severity-related components.

4.1 A disease-related axis dominated by glycerophospholipid loss and PLA2/LPCAT remodelling

The most robust finding of the study, lower plasmalogen p16:0/20:4, is consistent with recent evidence that glycerophospholipid and plasmalogen loss represents one of the more reproducible peripheral metabolic findings in schizophrenia (1, 9, 10, 48, 49). This includes the three-cohort lipidomic study by Tkachev et al., which reported reproducible decreases in PC and plasmalogen species across Russian, Chinese and German–Austrian cohorts (9), erythrocyte lipidomic data linking PC/PE plasmalogen loss to elevated PLA2 and LPCAT activity (36), cognitive associations of PE-plasmalogens in PsyCourse (49), cross-diagnostic lipidomic concordance across BD and schizophrenia (10), and glycerophospholipid/sphingolipid signatures in drug-naive schizophrenia (8).

The main mechanistic contribution of the present study is the gene-level convergence. Mapping altered metabolites to catalysing enzymes generated a 99-gene STRING subnetwork in which LPCAT4, PLA2G4A and LPCAT1 were among the highest Open Targets-ranked schizophrenia-associated enzymes and converged on phosphatidylcholine remodelling. This is consistent with the Lands cycle, in which PLA2-mediated deacylation and LPCAT-mediated re-acylation remodel the sn-2 fatty-acyl chain of glycerophospholipids[35–39]. Increased PLA2/LPCAT activity has been linked to phospholipid turnover, lipid peroxidation, ferroptosis and membrane stress (37, 39, 40). Independent CNV evidence implicating PLA2G4A in schizophrenia symptom dimensions[34], evolutionary and isozyme-level PLA2 analyses (38, 50), and the observed lowering of PC(16:0/18:2) and plasmalogen p16:0/20:4 together support PLA2/LPCAT remodelling as a plausible disease-related axis. These findings support targeted follow-up of a small phospholipid panel and motivate experimental testing of PLA2/LPCAT-linked mechanisms in schizophrenia-relevant cellular models (39, 40).

4.2 An antipsychotic-exposure-related axis involving mitochondrial fuel and isoprenoid metabolism

The CPZeq-high versus CPZeq-low contrast suggested an antipsychotic-exposure-related axis involving lower pyruvic acid, mevalonic acid, dimethyl-L-arginine and propionylcarnitine with increasing antipsychotic dose. This pattern is biologically coherent: pyruvate reflects mitochondrial fuel entry, mevalonate indexes cholesterol/isoprenoid synthesis, and dimethyl-L-arginine reflects nitric-oxide pathway regulation. These metabolites are compatible with downstream effects of mitochondrial complex-I inhibition, altered SREBP2 signalling or broader antipsychotic-associated metabolic stress.

This interpretation is consistent with recent pharmacological literature. Aripiprazole, brexpiprazole and cariprazine have been described as off-target mitochondrial complex-I inhibitors (26); second-generation antipsychotics disrupt ETC, TCA and glycolytic gene programmes (23, 24); aripiprazole affects mitochondrial polarisation and G6PDH activity (26); olanzapine alters lysosomal/autophagy and SREBP2-related pathways (29); clozapine activates an AhR–tryptophan–kynurenine–metabolic cascade with AMPK/HIF-1-related effects (31); and mTOR has been implicated in antipsychotic metabolic side effects (27). A registered risperidone versus aripiprazole trial measuring complex I, lactate and pyruvate will provide a prospective test of this axis (28).

The dimethyl-L-arginine finding is also relevant because asymmetric-dimethylarginine (ADMA) is elevated in schizophrenia meta-analysis [52]. In our cohort, dimethyl-L-arginine was not increased in the raw schizophrenia-control contrast but decreased with higher antipsychotic dose. One possible interpretation is that antipsychotic exposure modifies an underlying disease-related arginine/notric oxide pathway disturbance, consistent with DDAH-targeting and mGlu2/5–ADMA–NOS perspectives (52, 53). This interpretation remains exploratory and requires drug-naive and longitudinal replication.

4.3 A putative severity-related axis dominated by purinergic stress

Xanthine showed the clearest severity-related pattern in this panel: it was higher in the PANSS-high contrast but showed near-zero effects across smoking, antipsychotic class and CPZeq. This pattern supports xanthine as a candidate severity-associated marker rather than a diagnostic marker. The signal is consistent with purinergic literature implicating xanthine oxidoreductase in psychiatric oxidative stress [19–21, 55], allopurinol has been tested as an adjunctive purine-modulating strategy dies (20), dditional related evidence includes purine-salvage dysfunction and mitochondrial

effects (55–57), and the dependence of brain purine metabolism on salvage pathways and hypoxanthine pools (58). The upward movement of hypoxanthine in the schizophrenia-control contrast is consistent with the same xanthine-oxidoreductase axis. A small purinergic panel including xanthine, hypoxanthine, uric acid and allantoin should therefore be evaluated prospectively as a candidate symptom-monitoring panel.

The schizophrenia-only allantoin–PI(38:5) correlation links oxidative-damage and phospholipid- remodelling signals. Because allantoin reflects uric-acid oxidation by reactive oxygen species, this edge suggests possible coupling between purinergic stress and membrane remodelling in schizophrenia. This hypothesis remains exploratory and should be tested in a larger longitudinal cohort.

4.4 Strengths, limitations and interpretation caveats

The main strength of this study is its structured analytical design. All 171 metabolites were tested under panel-wide FDR control; sex, age and smoking were modelled as covariates; continuous clinical scales were analysed metabolite by metabolite; 12 case-vs-case deconfounding contrasts were used; and metabolite hits were mapped to enzymes, gene symbols and STRING interaction partners. The principal limitations are summarized in Table S5. The key caveats are the small sample size, sex–age imbalance, cross-sectional design, absence of a drug-naive cohort, targeted rather than untargeted metabolomics, and residual confounding by treatment, smoking, diet or metabolic state. Therefore, classifier performance and axis assignment should be interpreted as discovery-phase evidence, not clinical validation.

4.5 Comparison with prior studies and translational implications

Overall, our findings align with the dominant signals reported in schizophrenia metabolomics: glycerophospholipid loss in drug-naive and treated cohorts (1, 8–10, 12, 36); kynurenine-pathway shifts in first-episode, antipsychotic-naive, long-term treated, post-mortem and review datasets (13, 14, 16, 18, 59–61); purinergic and oxidative-stress abnormalities (19–21, 23, 58); and ADMA elevation (51). What distinguishes the present study is that these signals were not treated as one undifferentiated biomarker list but were organized into putative disease-, antipsychotic-exposure- and severity-related axes.

The gene-network convergence on PLA2/LPCAT enzymes is consistent with PLA2G4A CNV evidence (35). The antipsychotic-exposure-related pattern fits complex-I inhibition, clozapine-related AhR–tryptophan–kynurenine effects and prospective mitochondrial readouts in antipsychotic trials (26, 28, 31). The putative severity-related xanthine signal is consistent with broader purinergic-stress literature (19–21, 58). Two near-term translational directions follow: targeted replication of a minimal 5–7-metabolite panel measured by HILIC MRM, and longitudinal testing of the purinergic axis as a symptom-monitoring candidate. The analytical pipeline is also transferable to other psychiatric cohorts and is consistent with multi-omics and network-integration strategies (32–34, 62).

5. Conclusion

Targeted LC–MS/MS profiling of 171 plasma metabolites in this discovery cohort identified three partially separable metabolomic components in paranoid schizophrenia. The disease-related component was dominated by glycerophospholipid loss, with plasmalogen p16:0/20:4 remaining the only metabolite that survived age-, sex- and smoking-adjusted FDR correction and converging at the gene-network level on Lands-cycle enzymes, including LPCAT4, PLA2G4A and LPCAT1.

The antipsychotic-exposure-related component involved pyruvate, mevalonate and dimethyl-L-arginine, consistent with reports that several atypical antipsychotics can affect mitochondrial complex I and fuel metabolism. The putative severity-related component was centred on xanthine and related purinergic metabolites and was not primarily explained by smoking or CPZeq dose in this cohort.

Together, these findings support targeted replication of a focused metabolite panel including plasmalogen p16:0/20:4, PC(16:0/18:2), phosphorylcholine, pyruvate, mevalonate, dimethyl-L-arginine, xanthine and hypoxanthine in larger, longitudinal and drug-naive cohorts.

Declarations

Data and code availability

Raw and processed data supporting the conclusions are presented in the Supplementary information. The analysis can be reproduced using the documented Python code, data and parameter values provided in the Supplementary Methods.

Author contributions

P.I.B. contributed to the study conceptualization, performed the experimental work, analysed the data and contributed to the manuscript writing. M.K.L. performed the experimental work, analysed the data and contributed to the manuscript writing. M.A.S. performed the experimental work and contributed to the manuscript writing. D.Z.T. was responsible for the patient recruitment and clinical data collection. D.Kh.S. performed the experimental work and contributed to the manuscript review and editing. Z.F.K. coordinated the clinical part of the study and contributed to the manuscript review and editing. A.D.R. provided the analytical resources and contributed to the manuscript review and editing. S.N.M. contributed to the project coordination and the manuscript review and editing. D.N.S. provided the resources and contributed to the manuscript review and editing.

J.D. contributed to the study conceptualization, provided the resources, funding acquisition and contributed to the manuscript review and editing. V.N.B. provided the resources and contributed to the manuscript review and editing. E.A.E. supervised the study, contributed to the funding acquisition and the manuscript review and editing. N.V.B. supervised the study, contributed to the funding acquisition, wrote the manuscript, integrated the analytical and clinical results, critically revised the manuscript and prepared the final version for the submission. N.V.B. supervised the study, contributed data analysis conceptualization, funding acquisition and the manuscript review and editing. All authors reviewed and approved the final manuscript.

Funding

The study was conducted with support of Longhu Talent Project of Bengbu Medical University（NO. LH250101002); Anhui Province Jointly-Constructed Key Laboratory of Innovative Drugs Pharmaceutical Research and Clinical Evaluation; Talent Introduction Research Startup Fund of The First Affiliated Hospital of Anhui Medical University.

Conflicts of interest

The authors declare no conflicts of interest.

Ethics statement

This study was carried out in accordance with the Declaration of Helsinki. Ethical approval was received from the Local Ethics Committee of the Medical Academy of Kabardino-Balkarian State University named after H.M. Berbekov (expert conclusion No. 02.012, February 2, 2026).

Acknowledgments

The authors thank Mark M. Melamud for methodological assistance in data analysis.

Supplementary information is available at MP's website.

References

1. Modesti MN, Arena JF, Del Casale A, Gentile G, Borro M, Parmigiani G, et al. Lipidomics and genomics in mental health: insights into major depressive disorder, bipolar disorder, schizophrenia, and obsessive-compulsive disorder. Lipids in Health and Disease. BioMed Central Ltd; 2025. doi:10.1186/s12944-025-02512-x PubMed PMID: 40069786.
2. Song M, Liu Y, Zhou J, Shi H, Su X, Shao M, et al. Potential plasma biomarker panels identification for the diagnosis of first-episode schizophrenia and monitoring antipsychotic monotherapy with the use of metabolomics analyses. Psychiatry Res. 2023;321:115070. doi:10.1016/J.PSYCHRES.2023.115070 PubMed PMID: 36706560.
3. Konjevod M, Sáiz J, Bordoy L, Strac DS, Taha AY, Lanceros-Méndez S, et al. Validated metabolomic biomarkers in psychiatric disorders: a narrative review. Molecular Medicine. BioMed Central Ltd; 2025. doi:10.1186/s10020-025-01258-7 PubMed PMID: 40634860.
4. Yao G, Zeng J, Huang Y, Lu H, Ping J, Wan J, et al. Discovery of biological markers for schizophrenia based on metabolomics: a systematic review. Frontiers in Psychiatry. Frontiers Media SA; 2025. doi:10.3389/fpsyt.2025.1540260
5. Dong Y, Wang S, Qiu Y, Su Q, Sun X, Li M, et al. Plasma biomarkers in drug-naïve schizophrenia with severe cognitive impairment via targeted metabolomics. Psychoneuroendocrinology. 2026;184:107711. doi: 10.1016/J .PSYNEUEN.2025.107711 PubMed PMID: 41308587.
6. Couttas TA, Jieu B, Rohleder C, Leweke FM. Current State of Fluid Lipid Biomarkers for Personalized Diagnostics and Therapeutics in Schizophrenia Spectrum Disorders and Related Psychoses: A Narrative Review. Frontiers in Psychiatry. Frontiers Media S.A.; 2022. doi:10.3389/fpsyt.2022.885904
7. Wang Z, Wang Y, Jiang H, Chen L, Zhang X. Identification of Plasma Biomarkers in Untreated Schizophrenia Patients Using Untargeted Lipid Metabolomics. Neuropsychiatr Dis Treat. 2025;21:2721–32. doi:10.2147/NDT.S537721
8. Costa AC, Riça LB, van de Bilt M, Zandonadi FS, Gattaz WF, Talib LL, et al. Application of Lipidomics in Psychiatry: Plasma-Based Potential Biomarkers in Schizophrenia and Bipolar Disorder. Metabolites. 2023;13(5). doi:10.3390/metabo13050600
9. Tkachev A, Stekolshchikova E, Vanyushkina A, Zhang H, Morozova A, Zozulya S, et al. Lipid Alteration Signature in the Blood Plasma of Individuals With Schizophrenia, Depression, and Bipolar Disorder. JAMA Psychiatry. 2023;80(3):250–9. doi:10.1001/jamapsychiatry.2022.4350
10. Yin B, Cai Y, Teng T, Wang X, Liu X, Li X, et al. Identifying plasma metabolic characteristics of major depressive disorder, bipolar disorder, and schizophrenia in adolescents. Transl Psychiatry. 2024;14(1). doi:10.1038/s41398-024-02886-z PubMed PMID: 38531835.

11. Zhou M. MS analysis of the plasma metabolome reveals major changes of amino acid and energy metabolism for early-onset schizophrenia. Am J Transl Res. 2024;16(11):6423–34. doi:10.62347/idua6983 PubMed PMID: 39678582.
12. Golubova A, Stekolshchikova E, Gareeva A, Akhmerova I, Timerbulatov I, Zakurazhnaya V, et al. Blood Plasma Lipid Alterations Differentiating Psychotic and Affective Disorder Patients. Biomolecules. 2025;15(9). doi:10.3390/biom15091296 PubMed PMID: 41008603.
13. Li M, Wu Y, Xu Y, Huang X, Gao K, Hu N, et al. Peripheral tryptophan-kynurenine pathway dysfunction in first-episode schizophrenia. Sci Rep. 2025;15(1). doi:10.1038/s41598-025-86390-4 PubMed PMID: 39827210.
14. Kuuskmäe C, Philips MA, Kilk K, Haring L, Kangro R, Seppo I, et al. Kynurenine pathway dynamics in patients with schizophrenia spectrum disorders across the disease trajectory. Psychiatry Res. 2023;328:115423. doi: 10.1016/J .PSYCHRES.2023.115423 PubMed PMID: 37639988.
15. Brum M, Nieberler M, Kehrwald C, Knopf K, Brunkhorst-Kanaan N, Etyemez S, et al. Phase-and disorder-specific differences in peripheral metabolites of the kynurenine pathway in major depression, bipolar affective disorder and schizophrenia. The World Journal of Biological Psychiatry. 2023;24(7):564–77. doi:10.1080/15622975.2023.2169348
16. Antenucci N, D'Errico G, Fazio F, Nicoletti F, Bruno V, Battaglia G. Changes in kynurenine metabolites in the gray and white matter of the dorsolateral prefrontal cortex of individuals affected by schizophrenia. Schizophrenia. 2024;10(1):27. doi:10.1038/s41537-024-00447-3
17. Enes Inam M. The kynurenine pathway in major depressive disorder, bipolar disorder, and schizophrenia: a systematic review and meta-analysis of cerebrospinal fluid studies DOI: 10.47626/1516-4446-2022-2973/
18. Hatzimanolis A, Foteli S, Xenaki LA, Selakovic M, Dimitrakopoulos S, Vlachos I, et al. Elevated serum kynurenic acid in individuals with first-episode psychosis and insufficient response to antipsychotics. Schizophrenia. 2024;10(1). doi:10.1038/s41537-024-00483-z
19. Nelson KL, Voruganti VS. Implication of xanthine oxidoreductase in oxidative stress-related chronic diseases. Frontiers in Endocrinology. Frontiers Media SA; 2026. doi:10.3389/fendo.2025.1662037
20. Weiser M, Gershon AA, Rubinstein K, Petcu C, Ladea M, Sima D, et al. A randomized controlled trial of allopurinol vs. placebo added on to antipsychotics in patients with schizophrenia or schizoaffective disorder. Schizophr Res. 2012;138(1):35–8. doi:10.1016/J.SCHRES.2012.02.014 PubMed PMID: 22483162.
21. Cicero AFG, Fogacci F, Di Micoli V, Angeloni C, Giovannini M, Borghi C. Purine Metabolism Dysfunctions: Experimental Methods of Detection and Diagnostic Potential. International Journal of Molecular Sciences. Multidisciplinary Digital Publishing Institute (MDPI); 2023. doi:10.3390/ijms24087027 PubMed PMID: 37108190.
22. He Q, You Y, Yu L, Yao L, Lu H, Zhou X, et al. Uric acid levels in subjects with schizophrenia: A systematic review and meta-analysis. Psychiatry Res. 2020;292. doi:10.1016/j.psychres.2020.113305 PubMed PMID: 32702552.
23. Mortimer KRH, Katshu MZUH, Chakrabarti L. Second-generation antipsychotics and metabolic syndrome: a role for mitochondria. Frontiers in Psychiatry. Frontiers Media SA; 2023 doi:10.1111/jne.13347.
24. Panizzutti B, Bortolasci CC, Spolding B, Kidnapillai S, Connor T, Martin SD, et al. Effects of antipsychotic drugs on energy metabolism. Eur Arch Psychiatry Clin Neurosci. 2024;274(5):1125–35. doi:10.1007/s00406-023-01727-2
25. Fonseca M, Carmo F, Martel F. Metabolic effects of atypical antipsychotics: Molecular targets. J Neuroendocrinol. 2023;35(12):e13347. doi:https://doi.org/10.1111/jne.13347
26. Hardy RE, Chung I, Yu Y, Loh SHY, Morone N, Soleilhavoup C, et al. The antipsychotic medications aripiprazole, brexpiprazole and cariprazine are off-target respiratory chain complex I inhibitors. Biol Direct. 2023;18(1). doi:10.1186/s13062-023-00375-9 PubMed PMID: 37528429.
27. Zhuo C, Xu Y, Hou W, Chen J, Li Q, Liu Z, et al. Mechanistic/mammalian target of rapamycin and side effects of antipsychotics: insights into mechanisms and implications for therapy. Translational Psychiatry. Springer Nature; 2022. doi:10.1038/s41398-021-01778-w PubMed PMID: 35013125.
28. Shaju A, Mohapatra D, Mishra BR, Mishra A, Srinivasan A, Maiti R. Evaluation of atypical antipsychotic-induced mitochondrial dysfunction in patients with schizophrenia: a randomised controlled trial protocol. BMJ Open. 2025;15(10). doi:10.1136/bmjopen-2024-098173 PubMed PMID: 41093357.
29. Pozzi M, Vantaggiato C, Brivio F, Orso G, Bassi MT. Olanzapine, risperidone and ziprasidone differently affect lysosomal function and autophagy, reflecting their different metabolic risk in patients. Transl Psychiatry. 2024;14(1). doi:10.1038/s41398-023-02686-x PubMed PMID: 38191558.
30. Pereira S, Au E, Agarwal SM, Wright DC, Hahn MK. Antipsychotic-Induced Alterations in Lipid Turnover. Endocrinology. 2023;164(4):bqad025. doi:10.1210/endocr/bqad025
31. Fehsel K. Metabolic Side Effects from Antipsychotic Treatment with Clozapine Linked to Aryl Hydrocarbon Receptor (AhR) Activation. Biomedicines. Multidisciplinary Digital Publishing Institute (MDPI); 2024. doi:10.3390/biomedicines12102294
32. Sanches PHG, de Melo NC, Porcari AM, de Carvalho LM. Integrating Molecular Perspectives: Strategies for Comprehensive Multi-Omics Integrative Data Analysis and Machine Learning Applications in Transcriptomics, Proteomics, and Metabolomics. Biology. Multidisciplinary Digital Publishing Institute (MDPI); 2024. doi:10.3390/biology13110848 PubMed PMID: 39596803.

33. Szklarczyk D, Nastou K, Koutrouli M, Kirsch R, Mehryary F, Hachilif R, et al. The STRING database in 2025: protein networks with directionality of regulation. Nucleic Acids Res. 2025;53(D1):D730–7. doi:10.1093/nar/gkae1113 PubMed PMID: 39558183.
34. Ivanisenko VA, Gaisler E V., Basov N V., Rogachev AD, Cheresiz S V., Ivanisenko T V., et al. Plasma metabolomics and gene regulatory networks analysis reveal the role of nonstructural SARS-CoV-2 viral proteins in metabolic dysregulation in COVID-19 patients. Sci Rep. 2022;12(1). doi:10.1038/s41598-022-24170-0 PubMed PMID: 36404352.
35. Gao Z, Guo X, Sun Z, Wu S, Wang Q, Huang Q, et al. Copy number deletion of PLA2G4A affects the susceptibility and clinical phenotypes of schizophrenia. Schizophrenia. 2024;10(1). doi:10.1038/s41537-024-00474-0
36. Li M, Gao Y, Wang D, Hu X, Jiang J, Qing Y, et al. Impaired Membrane Lipid Homeostasis in Schizophrenia. Schizophr Bull. 2022;48(5):1125–35. doi: 10.1093/schbul/sbac011
37. Roggero A, Toyama MH, Sousa SF. Lands' Cycle at the Crossroads: Phospholipid Remodelling, Oxidative Stress, Cellular Toxicity, and Therapeutic Targeting. ACS Pharmacology and Translational Science. American Chemical Society; 2025. p. 3729–56. doi:10.1021/acsptsci.5c00482
38. Murakami M. The phospholipase A2 superfamily as a central hub of bioactive lipids and beyond. Pharmacol Ther. 2023;244:108382. doi: 10.1016/J
.PHARMTHERA.2023.108382 PubMed PMID: 36918102.
39. Lagrost L, Masson D. The expanding role of lyso-phosphatidylcholine acyltransferase-3 (LPCAT3), a phospholipid remodeling enzyme, in health and disease. Curr Opin Lipidol [Internet]. 2022;33(3). Available from: https://journals.lww.com/co-lipidology/fulltext/2022/06000/the_expanding_role_of_lyso_phosphatidylcholine.7.aspx
40. Li Z, Hu Y, Zheng H, Li M, Liu Y, Feng R, et al. LPCAT1-mediated membrane phospholipid remodelling promotes ferroptosis evasion and tumour growth. Nat Cell Biol. 2024;26(5):811–24. doi:10.1038/s41556-024-01405-y
41. Kay SR, Flszbeln A, Qpjer LA. The Positive and Negative Syndrome Scale (PANSS) for Schizophrenia [Internet]. Vol. 13. 1967. Available from: https://academic.oup.com/schizophreniabulletin/article/13/2/261/1919795
42. Overall John E, Gorham Donald R. The Brief Psychiatric Rating Scale. Psychol Rep. 1962;10(3):799–812. doi:10.2466/pr0.1962.10.3.799
43. Hobson J. The Montreal Cognitive Assessment (MoCA). Occup Med (Chic Ill). 2015;65(9):764–5. doi:10.1093/occmed/kqv078
44. Montgomery SA, Åsberg M. A New Depression Scale Designed to be Sensitive to Change. British Journal of Psychiatry. 2018/01/29. 1979;134(4):382–9. doi:DOI: 10.1192/bjp.134.4.382
45. Snaith RP, Hamilton M, Morley S, Humayan A, Hargreaves D, Trigwell P. A Scale for the Assessment of Hedonic Tone the Snaith–Hamilton Pleasure Scale. British Journal of Psychiatry. 2018/01/02. 1995;167(1):99–103. doi:DOI: 10.1192/bjp.167.1.99
46. Li K, Naviaux JC, Bright AT, Wang L, Naviaux RK. A robust, single-injection method for targeted, broad-spectrum plasma metabolomics. Metabolomics. 2017;13(10). doi:10.1007/s11306-017-1264-1 PubMed PMID: 28943831.
47. Naifar M, Ducatez F, Guidara W, Maalej M, Lesueur C, Pilon C, et al. Plasma Metabolic and Inflammatory Protein Signatures in Psychiatric Disorders. Int J Mol Sci. 2025;26(13). doi:10.3390/ijms26136260 PubMed PMID: 40650038.
48. Udagawa J, Hino K. Plasmalogen in the brain: Effects on cognitive functions and behaviors attributable to its properties. Brain Res Bull. 2022;188:197–202. doi:10.1016/J.BRAINRESBULL.2022.08.008 PubMed PMID: 35970332.
49. Oraki Kohshour M, Papiol S, Tkachev A, Stekolshchikova E, Adorjan K, Budde M, et al. Investigating the association of the plasma lipidomic profile with cognitive performance and genetic risk in the PsyCourse study. Transl Psychiatry. 2025;15(1). doi:10.1038/s41398-025-03323-5 PubMed PMID: 40155381.
50. Turnaev II, Bocharnikova ME, Afonnikov DA. Human phospholipases A2: a functional and evolutionary analysis. Vavilovskii Zhurnal Genet Selektsii. 2022;26(8):787–97. doi:10.18699/VJGB-22-95
51. Zinellu A, Tommasi S, Carru C, Sotgia S, Mangoni AA. A systematic review and meta-analysis of nitric oxide-associated arginine metabolites in schizophrenia. Translational Psychiatry. Springer Nature; 2024. doi:10.1038/s41398-024-03157-7 PubMed PMID: 39414767.
52. Vareltzoglou MR, Rodionov RN, Vernon AC, Bernhardt N. The Emerging Role of the DDAH Proteins in Psychiatric Disorders. Biological Psychiatry Global Open Science. 2025;5(6):100574. doi:10.1016/J.BPSGOS.2025.100574
53. Płoska A, Radulska A, Siekierzycka A, Cieślik P, Santocki M, Dobrucki IT, et al. The impact of mGlu2 or mGlu5 receptor activators on the production of l-arginine derivatives and the expression of PRMT5 or DDAH1 enzymes in animal models of cognitive decline. Nitric Oxide. 2025;154:140–51. doi:10.1016/J.NIOX.2024.11.010 PubMed PMID: 39638030.
54. Yao JK, Dougherty GG, Reddy RD, Keshavan MS, Montrose DM, Matson WR, et al. Homeostatic imbalance of purine catabolism in first-episode neuroleptic-naïve patients with schizophrenia. PLoS One. 2010;5(3). doi:10.1371/journal.pone.0009508 PubMed PMID: 20209081.
55. Flatow J, Buckley P, Miller BJ. Meta-analysis of oxidative stress in schizophrenia. Biol Psychiatry. 2013;74(6). doi:10.1016/j.biopsych.2013.03.018
56. Vinokurov AY, Soldatov VO, Seregina ES, Dolgikh AI, Tagunov PA, Dunaev A V., et al. HPRT1 Deficiency Induces Alteration of Mitochondrial Energy Metabolism in the Brain. Mol Neurobiol. 2023;60(6):3147–57. doi:10.1007/s12035-023-03266-2 PubMed PMID: 36802322.

57. Xu M, Tian P, Zhu H, Zou R, Zhao J, Zhang H, et al. Lactobacillus paracasei CCFM1229 and Lactobacillus rhamnosus CCFM1228 Alleviated Depression-and Anxiety-Related Symptoms of Chronic Stress-Induced Depression in Mice by Regulating Xanthine Oxidase Activity in the Brain. Nutrients. 2022;14(6). doi:10.3390/nu14061294 PubMed PMID: 35334950.
58. Sekine M, Fujiwara M, Okamoto K, Ichida K, Nagata K, Hille R, et al. Significance and amplification methods of the purine salvage pathway in human brain cells. Journal of Biological Chemistry. 2024;300(8). doi:10.1016/j.jbc.2024.107524 PubMed PMID: 38960035.
59. Marković M, Nikolić T, Totić-Poznanović S. The kynurenine pathway of tryptophan catabolism and schizophrenia. Medicinski podmladak. 2023;74(2):12–7. doi:10.5937/mp74-40330
60. Pocivavsek A, Schwarcz R, Erhardt S. Neuroactive Kynurenines as Pharmacological Targets: New Experimental Tools and Exciting Therapeutic Opportunities. Pharmacol Rev. 2024;76(6):978–1008. doi:10.1124/pharmrev.124.000239 PubMed PMID: 39304346.
61. Skorobogatov K, Autier V, Foiselle M, Richard JR, Boukouaci W, Wu CL, et al. Kynurenine pathway abnormalities are state-specific but not diagnosis-specific in schizophrenia and bipolar disorder. Brain Behav Immun Health. 2023;27:100584. doi:10.1016/J.BBIH.2022.100584
62. Kurbatov I, Dolgalev G, Arzumanian V, Kiseleva O, Poverennaya E. The Knowns and Unknowns in Protein–Metabolite Interactions. International Journal of Molecular Sciences. MDPI; 2023. doi:10.3390/ijms24044155 PubMed PMID: 36835565.

Figures

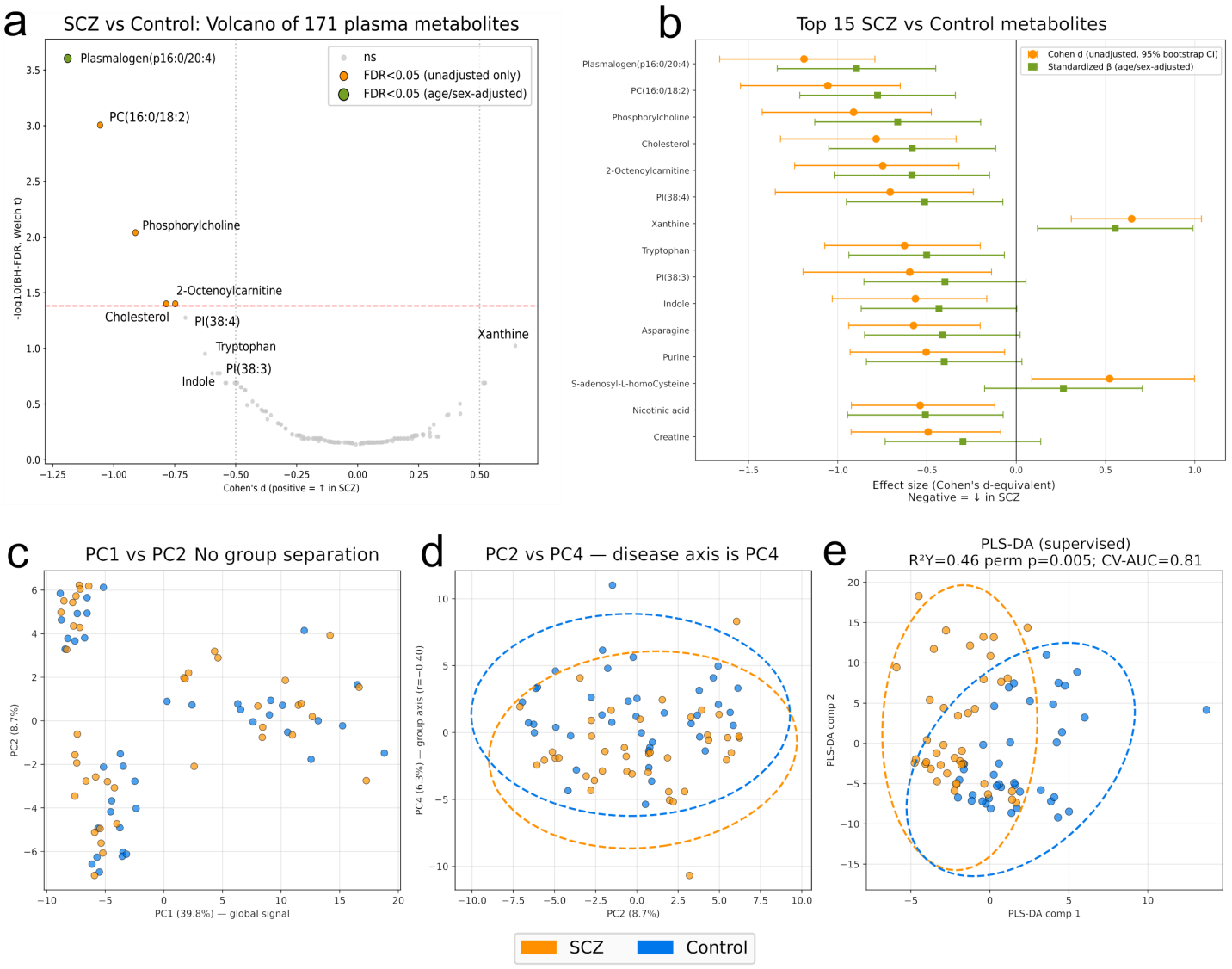
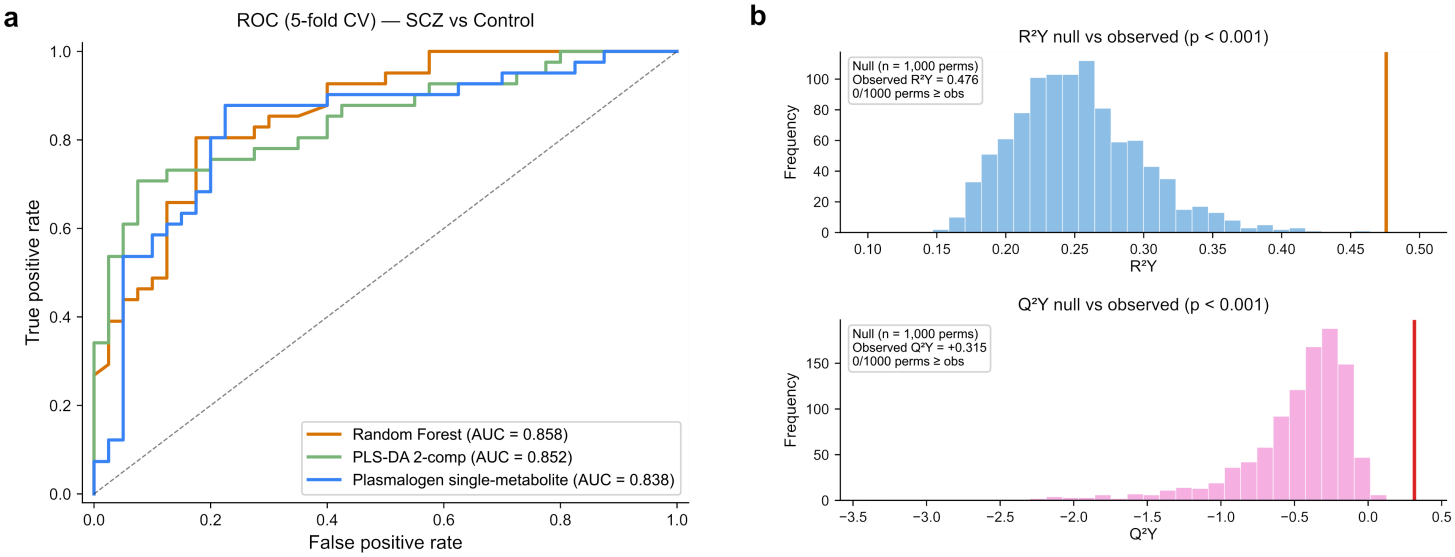


Figure 1

Univariate and multivariate metabolomic separation of schizophrenia and control plasma samples.

(a) Volcano plot of 171 plasma metabolites showing Cohen's d and −log10(BH-FDR); positive d indicates higher levels in schizophrenia. The dashed line denotes BH-FDR = 0.05. Plasmalogen p16:0/20:4 was the only metabolite surviving covariate-adjusted FDR correction. (b) Forest plot of the top metabolites ranked by adjusted FDR, showing raw Cohen's d with 95% bootstrap confidence intervals and covariate-adjusted standardised β. (c,d) PCA score plots of the Pareto-scaled metabolomic matrix: PC1 explained 39.8% of variance and PC4 contributed to group separation. (e) Two-component PLS-DA score plot for the 153-metabolite panel (R^2Y = 0.476; Q^2Y = 0.315; permutation p < 0.001). Orange indicates schizophrenia (n = 41) and blue indicates controls (n = 40); ellipses denote 95% group confidence intervals.



c

Model	Features	Mean AUC (5-fold CV)	± SD	Permutation *p* (1000×)
PLS-DA (2 components)	153	0.852	± 0.091	< 0.001
LASSO logistic (default λ)	65 (median)	0.852	± 0.052	< 0.001
LASSO logistic (sparse λ)	32 (median)	0.830	± 0.073	< 0.001
Random Forest (500 trees)	153	0.858	± 0.042	< 0.001
Univariate (Plasmalogen p16:0/20:4)	1	0.838	± 0.078	< 0.001

Figure 2

Cross-validated classifier performance for schizophrenia versus control discrimination.

(a) ROC curves for Random Forest (AUC = 0.858), two-component PLS-DA (AUC = 0.852) and plasmalogen p16:0/20:4 as a single-metabolite classifier (AUC = 0.838). (b) PLS-DA permutation test based on 1,000 label permutations for R^2Y and Q^2Y; both observed values exceeded the permutation null (p < 0.001). (c) Summary of classifier performance across models, showing mean 5-fold cross-validated AUC, standard deviation and permutation p value. Models were trained on the canonical 153-metabolite panel unless otherwise stated.

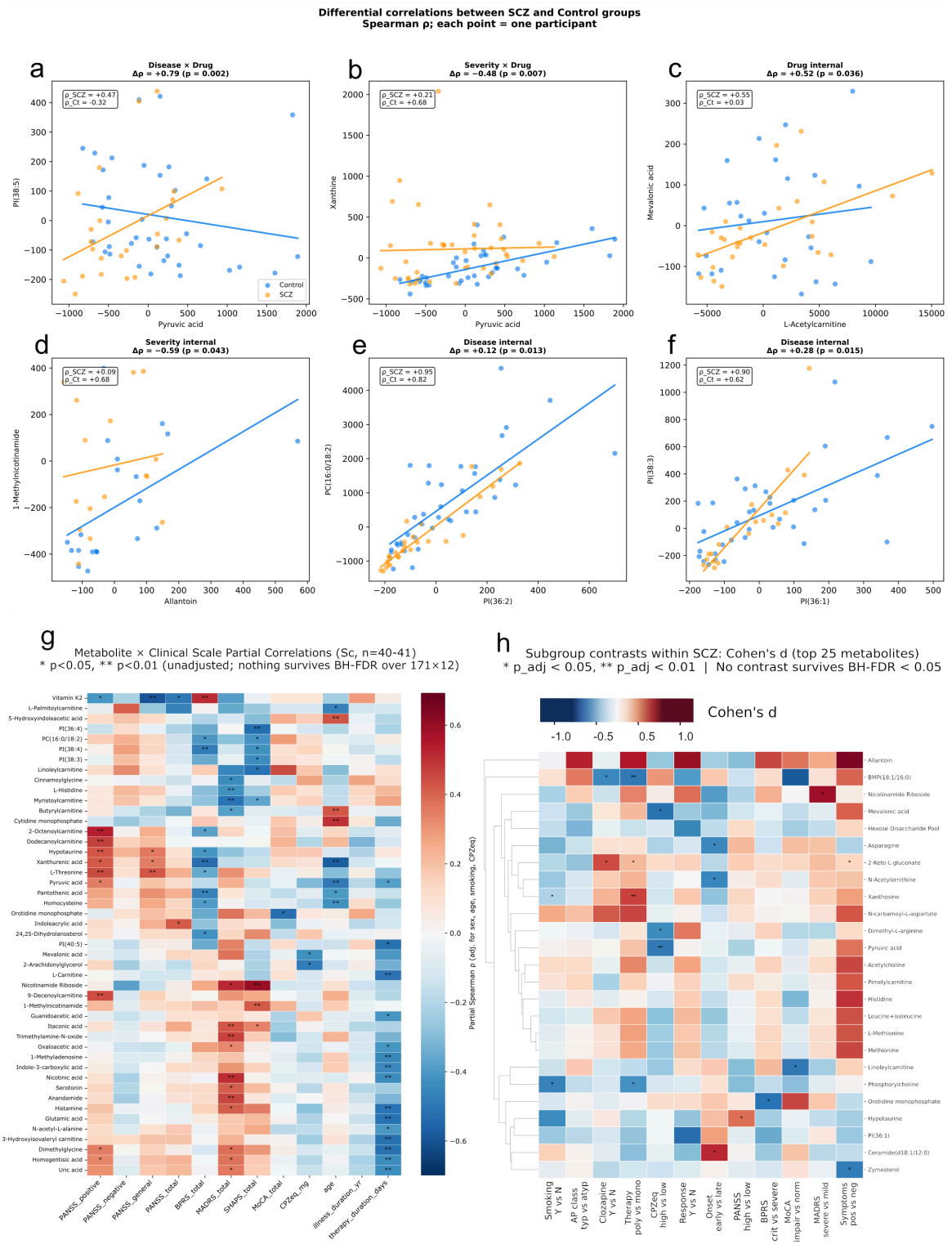


Figure 3

Differential correlations, clinical-scale associations and subgroup contrasts.

(a–f) Differential Spearman correlations between schizophrenia and control groups. Each point represents one participant; lines show group-specific regression fits. Δρ denotes ρSCZ − ρCtrl; p values were obtained using Fisher's z test. (a) PI(38:5)–pyruvic acid, Δρ = +0.79, p = 0.002. (b) Xanthine–pyruvic acid, Δρ = −0.48, p = 0.007. (c) Mevalonic acid–L-acetylcarnitine, Δρ = +0.52, p = 0.036. (d) 1-methylnicotinamide–allantoin, Δρ = −0.59, p = 0.043. (e) PC(16:0/18:2)–PI(36:2), Δρ = +0.12, p = 0.013. (f) PI(38:3)–PI(36:1), Δρ = +0.28, p = 0.015. (g) Partial Spearman correlations between metabolites and clinical variables within schizophrenia, adjusted for sex, age, smoking and, where appropriate, CPZeq dose. (h) Subgroup contrasts within the schizophrenia group, showing Cohen's d for selected metabolites across smoking-, treatment-, onset- and symptom-related contrasts. Rows were hierarchically clustered by effect-size profile. *p < 0.05; **p < 0.01.

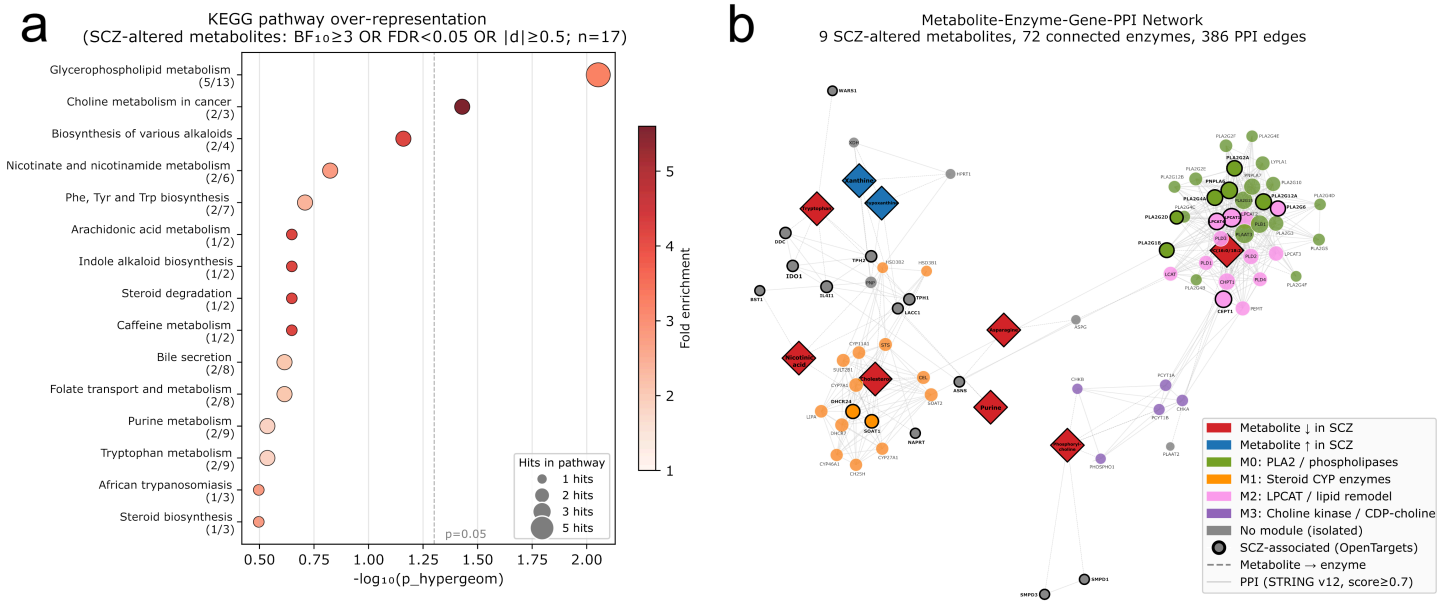


Figure 4

Pathway enrichment and metabolite-to-gene network.

(a) KEGG/SMPDB pathway over-representation analysis using the panel-detectable metabolite background (n = 126 mapped metabolites). Leading pathways included glycerophospholipid metabolism (KEGG map00564), choline-related metabolism, tryptophan-related pathways, arachidonic-acid metabolism and purine/caffeine-related pathways. (b) Metabolite → enzyme → gene STRING network constructed from altered metabolites. The network included 99 HUGO genes and 455 STRING edges at score ≥ 0.7. Gene nodes are coloured by OpenTargets schizophrenia association score. The highest-scoring phospholipid-remodelling genes included LPCAT4 (0.339), PLA2G4A (0.303) and LPCAT1 (0.300).

Supplementary Files

This is a list of supplementary files associated with this preprint. Click to download.

- BritTableS1.csv
- TableS4.docx
- TableS1.docx
- BritTableS2.csv
- BritSupplementaryMaterials.docx
- BritTableS3.xlsx
- TableS5.docx